

# Ring microfiber coupler erbium-doped fiber laser analysis

Azlan Sulaiman<sup>1\*</sup>, Sulaiman Wadi Harun<sup>1,2</sup>, and Harith Ahmad<sup>2</sup>

<sup>1</sup>Department of Electrical Engineering, Faculty of Engineering, University of Malaya, 50603 Kuala Lumpur, Malaysia

<sup>2</sup>Photonic Research Center, Department of Physics, University Malaya, 50603 Kuala Lumpur, Malaysia

\*Corresponding author: azlan27@gmail.com

Received October 24, 2013; accepted December 13, 2013; posted online January 23, 2014

A non-adiabatic microfiber coupler is fabricated by flame brushing technique and then theoretically and experimentally analyzed. The effective length of the microfiber coupler is determined by simulation, and a low-noise laser is demonstrated using various lengths of erbium-doped fiber (EDF) when incorporated in a laser setup. At 18.6-mW input pump power, the maximum output power of 20  $\mu$ W and the lowest lasing threshold of 3.8 mW are obtained with a 90-cm-long EDF.

OCIS codes: 140.0140, 060.0060, 190.0190.

doi: 10.3788/COL201412.021403.

Fiber lasers offer the benefits of long lifetime, low complexity, reduced running cost, and low maintenance. Thus, these lasers have important applications in the areas of optic communication, sensing, precision machining, material processing, ultra-fast diagnosis, biomedicine, and national defense<sup>[1–4]</sup>. Optical microfibers have recently become increasingly attractive because of their enabling optical properties, which include convenient connectivity to other fiberized components, strong optical confinement, and good flexibility<sup>[5,6]</sup>. Microfibers can be used to construct various devices including microfiber coupler (MFC), which has many potential applications, such as in high performance fiber lasers, fiber sensors, and optical communication systems<sup>[7–10]</sup>. For instance, Jung *et al.*<sup>[9]</sup> have demonstrated a broadband single mode bi-conical  $2 \times 2$  microfiber coupler with specifically designed transition regions that can effectively suppress any high-order mode present at the input fiber and provide efficient power splitting of the fundamental mode at the two output ports. In our early works, the MFC was used in generating dual-wavelength fiber laser by manually fabricating the transition section of the coupler taper to obtain a perfect filtering effect for dual wavelength laser<sup>[10]</sup>. In this letter, the microfiber coupler is used in generating compact, simple, and high performance laser, and is used to analytically and experimentally obtain the result involving the effective coupler length, analysis of configuration in getting low noise laser, and the relation between the length of the erbium-doped fiber (EDF) ring and laser wavelength.

Figure 1 shows an illustration of a standard bi-conical MFC that consists of two microfibers laterally touching each other. The MFC was manufactured by laterally fusing and tapering two twisted optical fibers, as shown in Fig. 2. In this letter, a small section of an appropriately twisted pair of bare single mode fibers was fused laterally with a suitably designed high-temperature flame using a flame brush technique. Motorized stages were used to pull the fiber during the heating process, and to move

a flame source. The fiber-pair is simultaneously pulled at a slow pace along their length to form a uniform, smooth, and slow taper, which is referred in literature as a bi-conical, tapered structure. The optical power of the monitoring signal, exiting from the two output fiber ports, was constantly recorded in real-time, throughout the fabrication process. The process was stopped at the point where an equal coupling ratio over the required wavelength range was obtained.

As an optical fiber is tapered down to a scale, such that the diameter of the fiber is comparable with the wavelength of the transmitted light, the fiber becomes a micro-scale diameter waveguide with an air cladding. Under these conditions, the coupling coefficient for a weakly fused MFC can be approximated by<sup>[7]</sup>

$$C(\lambda) = \frac{\pi\sqrt{n_1^2 - n_2^2}}{2\alpha n_1} e^{-2.3026(A+B\tau+C\tau^2)}, \quad (1)$$

where

$$A = \dots, B = \dots, C = \dots; a_1 = \dots, b_1 = \dots, c_1 = \dots; a_2 = \dots, b_2 = \dots, c_2 = \dots; a_3 = \dots, b_3 = \dots, c_3 = \dots;$$

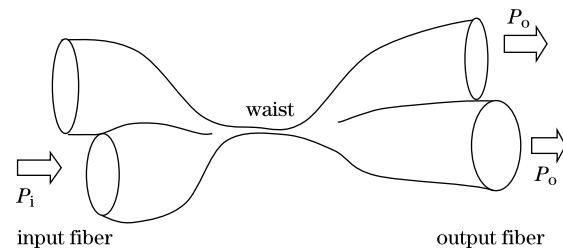


Fig. 1. Illustration of the bi-conical MFC.

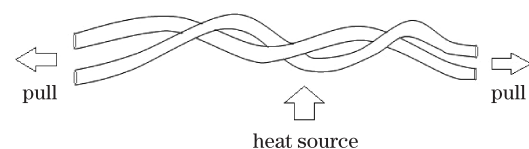


Fig. 2. Fabrication of the fused microfiber coupler using the flame brush technique.

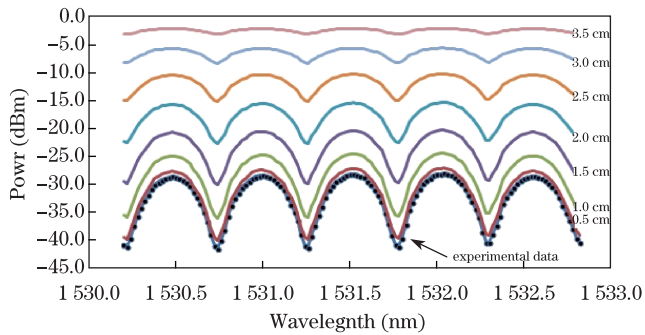


Fig. 3. Resonant spectra of MFC at various effective lengths  $L_{\text{eff}}$ .

$$\begin{aligned}
 A &= a_1 + a_2V + a_3V^2 & a_1 &= 2.2926 \\
 B &= b_1 + b_2V + b_3V^2 & b_1 &= -0.3374 \\
 C &= c_1 + c_2V + c_3V^2 & c_1 &= -0.0076 \\
 a_2 &= -1.591 & a_3 &= -0.1668 \\
 b_2 &= 0.5321 & b_3 &= -0.0066 \\
 c_2 &= -0.0028 & c_3 &= 0.0004
 \end{aligned}$$

$\lambda$  is the wavelength;  $n_1$  and  $n_2$  are the refractive index of the silica microfiber and the surrounding medium, respectively;  $a$  is the radius of the microfiber,  $\tau = d/a$ ,  $d$  is the distance between the axes of the fused microfibers;  $V$  is the normalized frequency, in which<sup>[7]</sup>

$$V = \left[ \frac{(2\pi a)}{\lambda} \right] (n_1^2 - n_2^2)^{1/2}. \quad (2)$$

The output power of the coupled port of the MFC is given by

$$P_o(\lambda) = P_i \cos^2(CL_{\text{eff}}), \quad (3)$$

where  $P_i$  and  $P_o$  are the input and the output powers, respectively, and  $L_{\text{eff}}$  is the effective coupling length.

Figure 3 shows the simulated resonance spectra of the non-adiabatic microfiber coupler based on Eqs. (1)–(3) at different effective lengths. The experimental result is also included in the figure at an effective length of 1.0 cm for comparison. The experimental spectrum obtained for 1.0 cm is close to the theoretical spectrum of 0.5 cm. This discrepancy between the theoretical and experimental results is due to the theoretical analysis, which assumed that the two fibers of MFC are arranged in parallel with uniform ideal cylindrical shape. In practice, the locations of these two fibers are not really parallel in the fabricated MFC because of the twisting step effect during the fabrication process. In addition, the non-uniformity in both transition area of the tapered regions and microfiber surface also contributed to the change in the effective length.

The LP01 mode of the input source transforms into cladding mode as the light travelling along the taper transition<sup>[11]</sup>. The large  $\Delta n$  between the cladding and air provide guidance to the input light in the taper waist. In the up-taper region, the mode is still guided by the air-cladding interface through the local modes of the multi-mode structure while exiting the coupler waist. These modes eventually overlap with the natural LP01

modes of the output fibers. However, given that the composite structure has a low taper inclination, i.e., the individual tapers being adiabatic<sup>[12]</sup>, only two lowest order super modes (even and odd) are excited in this multimode region. In a high-quality MFC with typical excess loss of less than 0.1 dB<sup>[11]</sup>, the excitation of higher order cladding modes is very low and negligible. In the coupling region, supermodes with different propagation constants provide a continuous change in the power distribution along the coupler cross section, resulting in a different power splitting at the output ports for different optical paths. The optical paths of the modes depend both on the coupling region length and its refractive index because both depend on the surrounding environment. For a given pair of single-mode fibers, some of the important parameters for fusion and tapering are the pulling speed, flame temperature, and flame brush width. These parameters dictate the performance of the fabricated couplers in terms of their optical characteristics.

In this letter, a compact and low noise EDF laser (EDFL) is demonstrated using an EDF loop attached to a microfiber coupler as a gain medium. Figure 4 shows the configuration of the proposed MFC-based EDFL, which consists of a loop of highly concentrated EDF, where a portion of the loop is fused together to form a microfiber coupler with a standard single mode fiber (Corning SMF-28) connected between the 980-nm pump and optical semiconductor amplifier (OSA). The flame brush technique is used in the fabrication of MFC as explained in the previous section. Figure 5 shows the microscope image of the fabricated MFC, which has a waist diameter and an effective length of approximately 5-6  $\mu\text{m}$  and 4 cm, respectively. The coupler is used for injecting the pump light and tap out the output to OSA for analysis. The results is compared with the conventional microfiber-based EDFL configuration<sup>[10,13]</sup>, where the A section in Fig. 4, connecting the 980-nm laser pump and microfiber devices, is replaced from SMF to 2-m EDF as a gain medium and microfiber structures to form a linear cavity. The performance of the laser is investigated for different perimeter lengths of the loop, ranging in length from 40 to 90 cm.

The fractions of the light propagated in the EDF ring through MFC provide 50:50 power splitting between the ring and the connecting single-mode fiber (SMF). The light circulation in the closed optical path forms the resonant cavity for the lasing operation. The EDF also acts as a gain medium that compensates the cavity losses in each round trip of the light. Fabricating MFC through fusing and tapering two optical fibers enables an exchange of optical power between the two fibers. Jung *et al.*<sup>[9]</sup> has concluded that the thinner the MFC ( $< 1.5 \mu\text{m}$ ), the more it is efficient

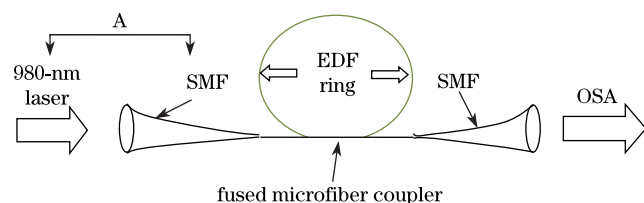


Fig. 4. Configuration of the proposed MFC based EDFL.

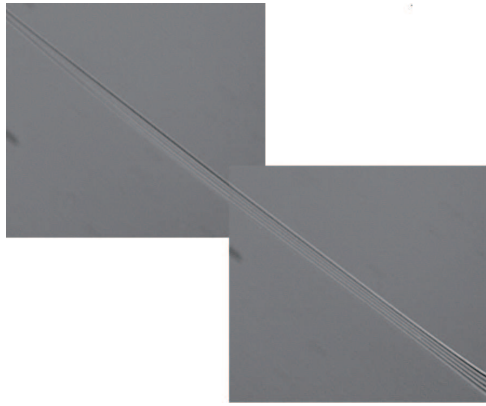


Fig. 5. Microscope image of the microfiber coupler.

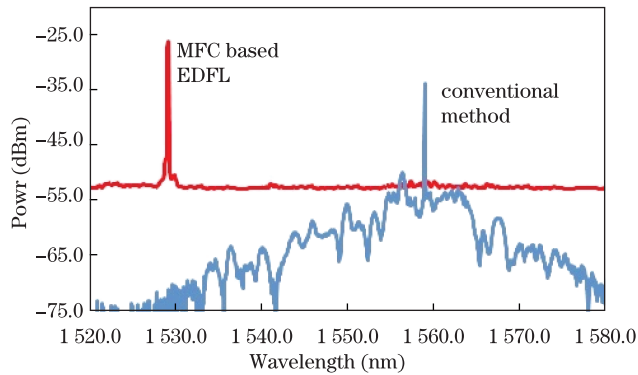


Fig. 6. Lasing characteristic comparison between the newly enhanced method (MFC-based EDFL) and the conventional method.

in providing power splitting (50:50) into the fundamental mode at the coupler port. The bi-conical transition of the MFC region provides effective optical filtering that suppresses higher-order modes and provides efficient power splitting into the fundamental mode at the connecting fiber and the EDF ring. When the pump power is increased above the lasing threshold, the lasing peak is observed operating at 1529.2 nm, with  $-26.23$ -dBm output power. In addition, the laser is stable at room temperature, with optical signal-to-noise ratios (OSNR) of 26.18 dB, as shown in Fig. 6. The lasing wavelength shown in Fig. 6 is determined by EDF gain, cavity loss, and optical filtering characteristics by MFC. The laser is considered a single mode because of the optical filtering characteristic of MFC, specifically at the tapered fiber, which capable of suppressing higher-order mode wave. The insertion loss observed between both configurations is about 7.56 dB at the highest peaks. The amplification of spontaneous emission (ASE) is generated for both methods in different shapes with different noise levels. MFC-based EDFL has shown constant power levels for the entire wavelength between 1520 and 1580 nm of  $-51.4$  dBm, and the noise figure approximately ranges from 0.2 to 0.5 dB compared with the conventional method, showing obvious intensity noise approximately 10 dB. Intensity noise was partly sourced from quantum noise associated with thermal fluctuation in the gain medium. The MFC-based laser uses a short

EDF (less than a meter) as a gain medium, which explained the reason behind the low noise figure.

Figure 7 shows the single-mode laser output versus pump power. The lasing threshold for the conventional configuration (4 mW) is lower compared with that of the MFC-based EDFL (5.5 mW), whereas the slope efficiency of the MFC-based EDFL was higher (0.006%) compared with that of the conventional method (0.0048%) when the input pump (15 mW) is applied. Compared with the linear cavity of the conventional method, high slope efficiency can easily be achieved by MFC EDFL although the threshold pump power is slightly higher. Optimizing the EDF length and reducing the cavity loss are the ideas to make the EDFL operate in deep saturation<sup>[14–16]</sup>.

Figure 8 shows the laser spectra of the proposed MFC-based EDFL at various ring lengths, ranging from 40 to 90 cm. The ASE resonated and amplified inside the ring to generate the laser, whereas a fraction of the laser resonated through MFC 50:50 power splitting directly to the output port. The longer the EDF ring, the longer the operating lasing wavelength and the lasing determined by the filtering characteristic of MFC, EDF gain, and cavity loss. With 17-mW pump power, the highest SNR is 35.2 dB belonging to the 70-cm ring, and the lowest is  $-20.7$  dB, which belong to 50-cm length. Although the effective length of the MFC is about 4 cm for all ring lengths, the quality of the fabricated MFC is different among each other.

In conclusion, a low noise EDFL operating at 1526 is demonstrated in assistance of a non-adiabatic microfiber coupler. At the cavity length of 90 cm, the EDFL starts to lase at the pump power of 3.8 mW and produces the maximum output power of  $20 \mu\text{W}$ , with a SNR of 26 dB at the pump power of 18.6 mW.

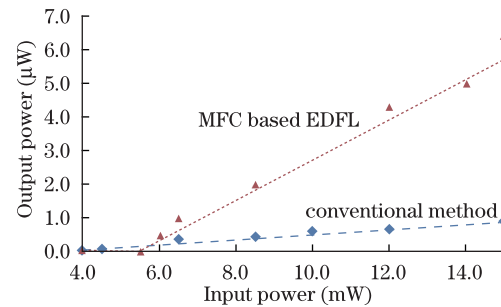


Fig. 7. Pump power characteristic.

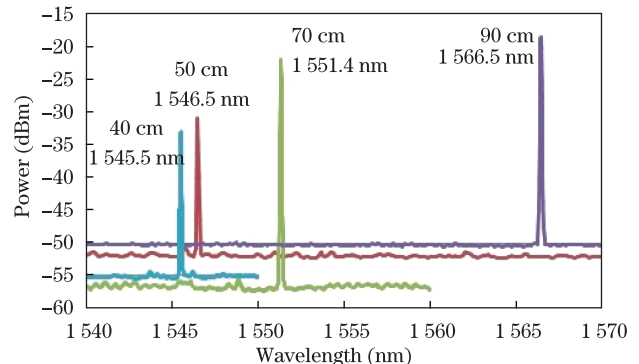


Fig. 8. Lasers produced with various EDF ring lengths at 17.0-mW pump power.

This work was supported by the University of Malaya Research Grant Scheme under Grant No. PG139-2012B.

## References

1. J. Yang, Y. Tang, J. Xu, *Photon. Res.* **1**, 52 (2013)
2. R. Tao, X. Wang, H. Xiao, P. Zhou, and L. Si, *Photon. Res.* **1**, 186 (2013).
3. Rene Platz, Gotz Erbert, Wolfgang Pittroff, Moritz Malchus, Klaus Vogel, and Gunther Trankle, *High Power Laser Sci. Eng.* **1**, 60 (2013).
4. S. J. Tan, S. W. Harun, H. Arof, and H. Ahmad, *Chin. Opt. Lett.* **11**, 073201 (2013).
5. Z. Wei, Z. Song, Z. Zhang, Y. Yu, and Z. Meng, *Chin. Opt. Lett.* **11**, 110602 (2013).
6. Y. Yu, L. Jiang, B. Li, Z. Cao, and S. Wang, *Chin. Opt. Lett.* **11**, 110603 (2013).
7. L. Bo, P. Wang, Y. Semenova, and G. Farrel, *IEEE Photon. Technol. Lett.* **25**, 228 (2013).
8. M. Ding, P. Wang, and G. Brambilla, *Opt. Express* **20**, 5402 (2004).
9. Y. Jung, G. Brambilla, and D. J. Richardson, *Opt. Express* **17**, 5273 (2008).
10. A. Sulaiman, S. W. Harun, M. Z. Muhammad, and H. Ahmad, *IEEE J. Quantum Electron.* **49**, 586 (2013).
11. K. Okamoto, *Fundamentals of optical waveguides* (Academic Press, San Diego, 2000) pp. 323.
12. J. D. Love, *Electron. Lett.* **23**, 993 (1987).
13. A. Sulaiman, S. W. Harun, F. Ahmad, S. F. Norizan, and H. Ahmad, *Laser Phys.* **22**, 588 (2012).
14. X. Dong, N. Q. Ngo, and P. Shum, *Opt. Express* **11**, 1689 (2003).
15. A. Bellemare, M. Karasek, C. Riviere, F. Babin, G. He, V. Roy, and G. W. Schinn, *IEEE J. Select. Top. Quantum Electron.* **7**, 22-29 (2001).
16. M. Mignon and E. Desurvire, *IEEE Photon. Technol. Lett.* **4**, 850 (1992).